Optimization of fixed bed column process for removal of Fe(II) and Pb(II) ions from thermal power plant effluent using NaoH-rice husk ash and *Spirogyra.*

M.D. Yahya [a], I.B. Muhammed [a], K.S. Obayomi [b],*, A.G. Olugbenga [a], U.B. Abdullahi [a]

[a] *Department of Chemical Engineering, Federal University of Technology Minna Niger State, Nigeria*
[b] *Department of Chemical Engineering, Landmark University Omu-Aran Kwara State, Nigeria*

ARTICLE INFO

ABSTRACT

This study was carried out to investigate and optimize the potentials of green algae (*spirogyra*) supported with treated NaOH- rice husk ash in a fixed bed column for the removal of Fe(II) and Pb(II) ions from a thermal power plant effluent. The optimization was done with central composite design using the Design Expert 10.0.0 software. The effluent was characterised using atomic absorption spectrophotometer with initial concentration values of 17.9 and 4.95 mg/l for Fe(II) and for Pb(II) ions respectively. The developed rice husk-spirogyra adsorbent was characterized using proximate analysis, SEM, BET, FTIR and TGA. The results from the proximate analysis gave a moisture content of 13%, bulk density of 0.347 g/cm^3, loss of mass ignition of 2.2 g, pH of 6.97 and pH point of zero charge (pH-pzc) of 4.94. The SEM images revealed an adsorbent with numerous pores, cavities and an irregular rough surface. The FTIR showed the O−H, $C = O$ and C−O functional groups as being responsible for the adsorption of the heavy metal ions. The BET analysis revealed high surface area of 534.414 m^2/g with pore volume of 0.3219 cm^3/g and pore size of 2.810 nm which reduced drastically to a surface area of 375 m^2/g after adsorption. For the column sorption study, the effects of bed height, (5, 10 and 20 cm), at flow rate, (3, 6, and 9 ml/min), and initial concentrations of Fe(II) (17.9, 10.23, and 5.53 mg/L) and Pb(II) (1.65, 3.1, and 4.95 mg/L) established that an increase in bed heights, reduced flow rates and inlet concentrations gave over 48.3 and 58.30% removal of the Fe(II) and Pb (II) ions which had a significant effect on the breakthrough and exhaustion time. The data were subjected to kinetics isotherms with the Clark model given the best fit with R^2 values of 0.9643 for Fe(II) and 0.9594 for Pb(II) ions.

* Corresponding author
E-mail address: obayomi.kehinde@lmu.edu.ng (K.S. Obayomi).

Introduction

Scientific research in recent time has shown increased emphasis on the adverse effect of heavy metals on human health [1,2,3,4]. The effect of toxic high-density metals includes skin cancer, neurological damages, pulmonary diseases and hypertension [5]. Effluent from process industries such as pharmaceuticals, textiles, paints, power plant, and battery are largely responsible for these toxic heavy metals presence in our water resources [6]. Health governing bodies like World Health Organization (WHO) and the United States Environmental Protection Agency (EPA) have set very strict limit on the level of these heavy metals in our freshwater. The EPA criterion for acceptable level of Pb (II) and Fe(II) in water are 0.1 mg/L and 1.0 mg/L respectively (EPA. 2018). There is therefore a need for the industrial effluents to be effectively treated before being discharged into the water bodies. Several methods for treatment exist; these include chemical precipitation [7–8], ion exchange [9]. These treatments are not cost effective and are not efficient in the removal of low concentration of heavy metals from water [10].

Cheap, environmentally friendly and effective treatment process using readily available materials is focused on in the treatment of industrial effluents [11]. Biosorption is one of such low cost treatment process. It can be defined as the property of a certain type of inactive, non-living biomass to bond and concentrate heavy metals from even very dilute solutions [5,12]. Biomass that exhibits this property is known as biosorbent, and this has high heavy metal removal capacity. A key condition in selecting suitable biomass is the availability, renewability, cheap and easily accessible. Examples of biosorbents used in previous researches include kolanut pod [13], cotton hulls [14], sugar cane bagasse, yeast biomass, and sorghum. Other readily available biomass of particular interest includes the green algae and rice husk.

Heavy metal-ion adsorption using biological sources such as algae, fungi, bacteria, fruits, vegetables and aquatic organism has attracted great attention due to their low cost, effective adsorbents and high efficiency [15,16] reported on the efficiency of chitosan-algae biomass composite microbeads for heavy metal removal. One of the research focused biological source is algae. Algae contains chitin, lipids, polysaccharides and protein in its cell walls. These macromolecules are made up of different functional groups as carboxyl, carbonyl, hydroxyl and phenolic hydroxyl. During adsorption these sets of functional groups form coordination complexes with heavy metals, this enable effective adsorption to take place. Algae is widely used as an ideal and promising adsorbent because of its following characteristics: its availability, low cost, rapid biosorption capability, high efficiency, reusability, high selectivity and absence of toxic waste generation [16]. Brown algae is considered to be versatile, low cost, effective adsorbents. It does not require any special treatment in its preparation process and has a relatively large surface area with high binding affinity compared to other materials [17,18,19]. Amongst the algae, the green algae: *Spirogyra species* which is an un-branched green filamentous biomass has been reported by [20] and [21] to have high heavy metal removal capacity. Rice husk is also reported by [22, 23] and [24] to have good heavy metal removal capacity.

This study was carried out to investigate high performance and high removal capacity of combining two effective adsorbents i.e. NaoH-rice husk and spirogyra for the removal of Fe(II) and Pb (II) ions from thermal power plant effluent. Several authors such as [22],[23] and [24] reported on synthesis of composite snail shell-rice husk adsorbent for brilliant green dye uptake from aqueous solution; however, they did not consider the optimization of the process parameters and the use of a fixed bed column to treat the effluent.

This study would concentrate on the optimization of the NaOH-rice husk ash and *spirogyra Africana czurda* process parameters using experimental design tools to study the activation temperature, time, mixing ratio and removal efficiency of Fe (II) and Pb (II) ions in thermal power plant effluents using a fixed-bed column.

Methodology

Pretreatment of rice husk and spirogyra

5 g of rice husk was mixed in 95 mL of 3% NaOH (aqueous solution) in a 250 mL volumetric flask and heated at 120 °C for 35 min. The treated rice husk was then filtered and washed with demineralized water; it was then dried and stored for further analysis [18]. Distilled water was used to wash the *spirogyra* to enhance purification. The spirogyra was collected from small streams around Ajaokuta thermal plant, Nigeria. It was then dried at 25 °C for 48 h before use [21].

Characterization of the thermal power plant effluent

The thermal power plant effluent was collected from a thermal power plant in Ajaokuta, Kogi state. Nigeria. The heavy metal concentration of the thermal power plant effluent was determined using the atomic absorption spectrophotometer. The AAS technique makes use of the wavelengths of light specifically absorbed by an element. The sample is fed into the nebulizer where it was bombarded by light waves, the monochromator detects the number of photons emitted and transforms this data into metals concentrations present in the sample.

Table 1
Independent Factors, their Minimum and Maximum Levels for the Central Composite Design.

Factors	Code	Units	$-\alpha$	-1	0	$+1$	$+\alpha$
Activation Temperature	X_1	^{0}C	203.24	431.80	767.10	1102.40	1330.94
Time	X_2	hrs	0.25	0.32	4.08	6.36	7.91
Mixing ratio	X_3	-	6:1	5:1	1.5:1	1:1.7	1:4

Characterization of the rice husk-Spirogyra

Thermo gravimetric analysis (TGA) of rice husk-spirogyra

The TGA analysis of the sample was done using PerkinElmer TGA 4000 instrument. A 0.5 g of the sample was placed into the holder via the top loading pan and covered. Nitrogen gas was supplied to purge the system and its flow rate was set to 50 ml/min before analysis was conducted. Data generated were captured and reported accordingly.

Determination of Bet surface area and pore volume of rice husk-Spirogyra adsorbent

The BET analysis gives the surface area, pore size and pore volume of the sample. The Quantachrome Instruments Nova 3200e surface area analyzer was used to analyze the sample. This was done to study the rice husk – spirogyra surface area before and after adsorption.

Scanning Electron Microscopy (SEM) of the adsorbent

This SEM analysis was carried out according to the method reported by [19] where an ASPEX 3020 scanning electron microscope, model SIRIUS50/3.8 with an attached energy dispersive X-ray spectroscopy (SEM/EDX) machine was used to generate images of the rice husk – spirogyra sample. The machine was operated at an accelerated voltage of 5 to 15 kV to determine the chitin samples elemental composition. The SEM analyses were done to determine the morphology of the adsorbent. This was done before and after the column adsorption experiment.

Analyses of the Fourier Transform Infrared Spectroscopy (FTIR) of the adsorbent

This was carried out in accordance to the method reported by [19] where the adsorbent was air-dried at 80 °C for 10 h, followed by 105 °C for 1 h after which it is cooled in a desiccator with CaO. The FT-IR spectra was obtained by feeding the dry adsorbent sample into an Impact 360 FT-IR spectrometer under dry air at room temperature using KBr pellets.

Preparation of Rice Husk (RH)-Spirogyra biosorbent

The range and levels of the process conditions (mixing ratio, activation temperature, and time) for producing the composite RH-*spirogyra* biosorbent samples was obtained from the result of Central Composite Design (CCD) using Design Expert 10.0.0 software® as shown in Table 1. Each mixture was prepared at different mixing ratio, activation temperature and time.

Adsorption studies

A column adsorption studies was adopted to investigate the efficiency of the adsorbent. It was done in a glass horizontal column of 2 cm internal diameter and 50 cm height. A peristaltic pump was used to maintain steady flow rate. To prevent adsorbent loss glass wool was placed underneath at the bottom of the column. The study was investigated at room temperature at a bed height (5, 10 and 20 cm), flow rate (3, 6and 9 ml/min) and initial concentration (17.7, 10.23 and 5.27 mg/L). Samples were taken every 2 h from the bottom of the glass column and analyzed with Atomic absorption spectrophotometer (AAS) was carried out to test for Fe(II) and Pb(II) concentration.

Results and discussion

Physicochemical properties of the materials

In adsorption studies, parameters such moisture content, loss of mass ignition, bulk density, pH and point of zero charge (pHpzc) are usually good indicators of whether a material is a viable adsorbent. Therefore, characterization of the rice husk-spirogyra adsorbent used to study the removal efficiency of Pb and Fe ion in thermal power plant effluent was carried out in this study.

Moisture content

A viable adsorbent material is usually moisture free or contains very little moisture. The lower the moisture the more viable the adsorbents, the acceptable limit of moisture allowed in materials is usually within 3–6% according to ISI standards. The modified rice husk properties were compared to the values obtained in literature and the results are presented in Table 2.

Table 2
The Properties of the modified rice husk.

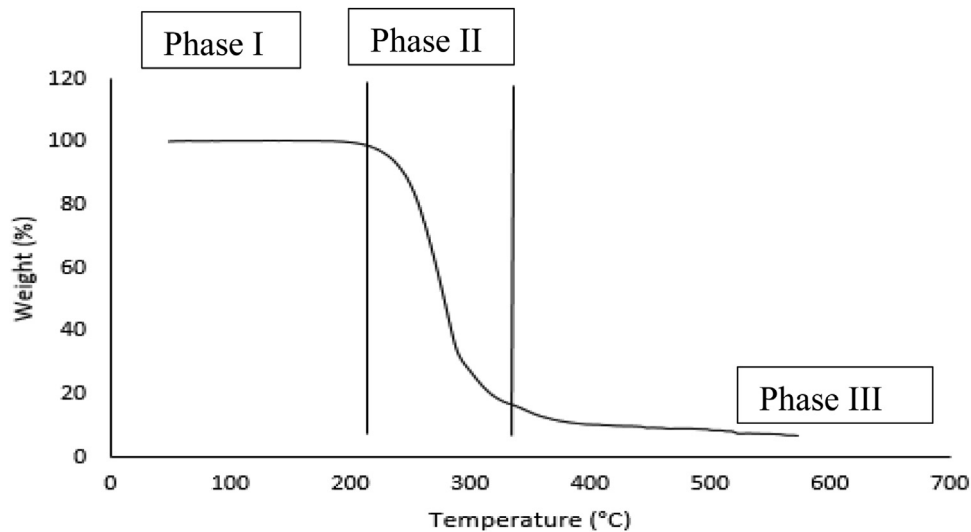| Properties	Modified rice husk	Literature value of rice husk
Moisture content (%)	13.000	12.000
Loss of mass ignition (g)	2.200	0.900
Bulk density (g/cm^3)	0.347	0.386
pH	6.970	7.000
pHpzc	4.950	4.670

Fig. 1. TGA Analysis of the adsorbent.

However, materials with moisture content within the ranges of 1–20% have been reported by [20] to still be viable adsorbent material. Therefore, rice husk-spirogyra adsorbent with a moisture content of 13% is still a viable adsorbent for effluent treatment.

The point of zero charge (pHpzc)

The point of zero charge values is another characteristic that is used in identifying the right sorption material for removal of heavy metal. Materials with low point zero charge would be highly effective in removing heavy metals that possess positive ions, while materials with high pHpzc values would be best to remove negative ions [22].

TGA analysis

The TGA analysis of Fig. 1 at phase I varied between 0 and 100 °C and thus, corresponds to the loss of moisture content; the rice husk has low moisture content hence the slight drop in the curve. In phase II from 220 to 510 °C showed the loss of volatile component, in this phase the sharp drop of the curve indicates that all the volatile components have evolved and organic matter decomposed from the heat treatment. From phase III, the straight line indicates that only carbon is left at a temperature of 510 °C. Hence from the result, thermal activation of rice husk temperature must be greater than 510 °C [23].

BET characterization of Rice Husk-Spirogyra

The surface area, pore volume and pore size before and after adsorption was carried out using the Barret- Joyner- Halenda method (BJH). A surface area of 657.7 m^2/g indicates the material has very high surface area and this can be attributed to the chemical pretreatment and optimization of the adsorbent. From the values after the adsorption there was a slight reduction in pore volume from 0.3219 to 0.2000 cm^3/g and pore size (2.138 to 2.132 nm) but larger reduction in surface areas of 408.7 m^2/g indicated that the adsorbent material pore spaces have been filled to some extent.

FTIR spectra analysis

Fig. 2 & 3 showed the peaks of the rice husk-spirogyra adsorbent and it reflect the complex nature of rice husk. The largest peaks of wave number 3447.91 cm^{-1} correspond to O–H group; this could be present in the carboxylic acid on the rice husk surface. The other peaks identified include 1654.09–1636.91 cm^{-1} which corresponds to the C–H functional group, 1458–1419.68 cm^{-1} to the $C = O$ group, while 1096–468.28 cm^{-1} corresponds to the C–O group. The hydroxyl group O–H acts as a proton donor and can be said to be capable of adsorbing heavy metal ions. Fig. 3 shows a shift in the O–H band, the bands of C–H and C–O also showed shifts while the $C = O$ disappeared. These changes could be attributed to the surface
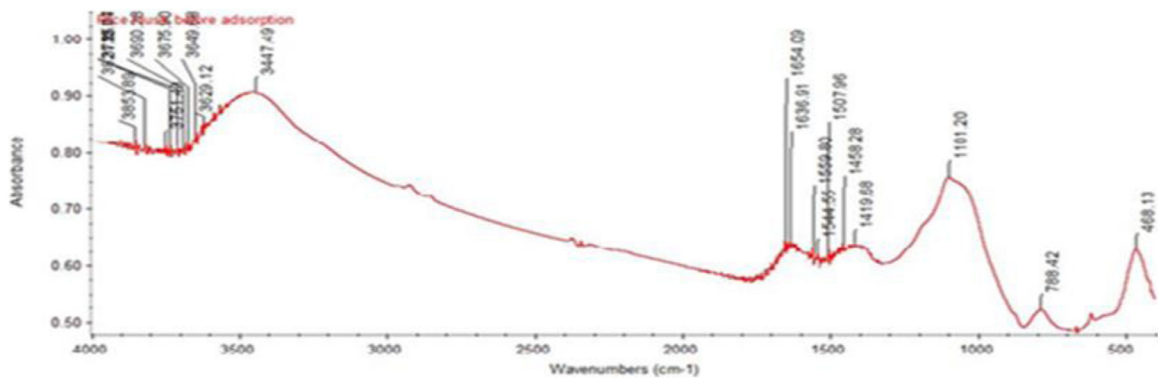
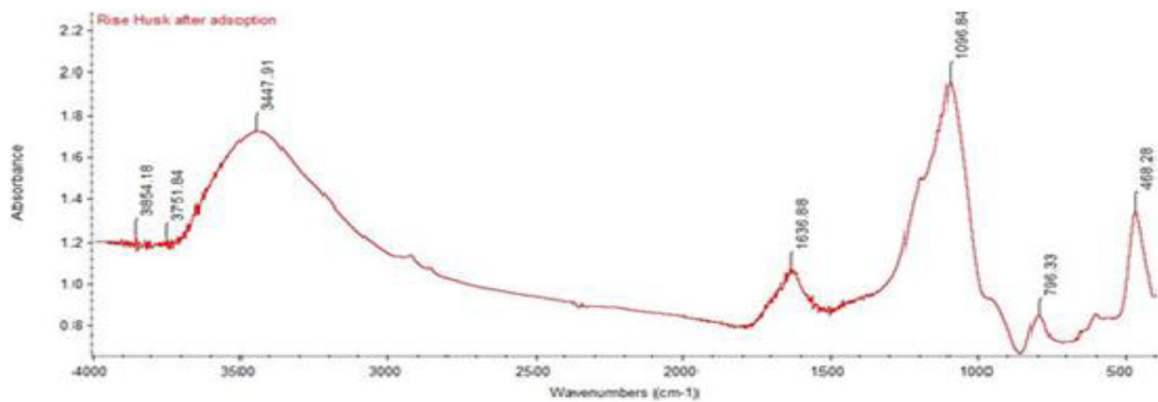**Fig. 2.** FTIR of the Rice Husk-Spirogyra before Adsorption.

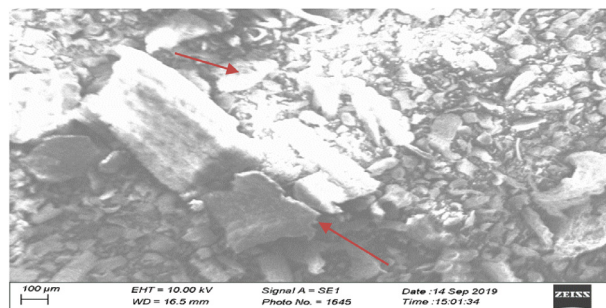**Fig. 3.** FTIR of the Rice Husk-Spirogyra after Adsorption.

Fig. 4a. SEM of Rice Husk-Spirogyra adsorbent before adsorption

complexaion between Pb and Fe with the hydroxyl and carboxylic groups indicating that chemical complexation may be responsible for adsorption [24].

SEM surface morphology

The surface morphology of the rice husk- spirogyra adsorbent was examined using Scanning Electron Microscopy (SEM) as shown in Fig. 4a& b. SEM analysis was conducted at two different magnifications for rice husk – spirogyra; before adsorption and after adsorption, in an attempt to observe the surface structure and any changes that could occur due to adsorption on its surface. The micrographs obtained as shown in Fig. 4a, indicated the changes in surface texture and pore development. There were white crystalline irregular rough surface which is the results of the developed RH-S. This created pores and cavities are responsible for the adsorption of the Pb (II) and Fe (II). Fig. 4b showed that the micrographs obtained had no clear pore spaces but swellings, which may be due to agglomeration of the Pb (II) and Fe (II) on the pore sites. The EDX analysis showed high concentration of K, Na and Si which is the results of the changes in the cell wall that consist of polysaccharides especially pectin [25]. However, after the adsorption there were significant reduction in Si and Na detected
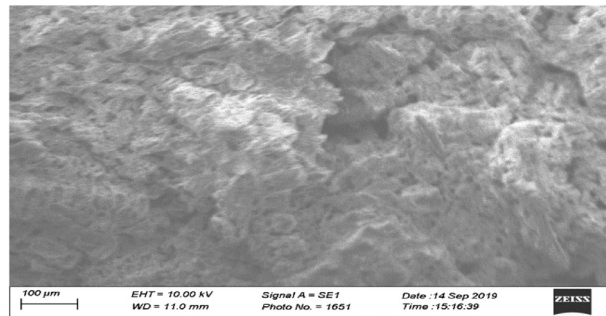
Fig. 4b. SEM of Rice Husk-Spirogyra adsorbent after adsorption.

Table 3
Factors of Experiment in Coded Units as well as Actual Units and their Responses.

Run	Factor 1 A:Activation Temperature °C	Factor 2 B:Time hours	Factor 3 C:Mixing Ratio	Response 1 Pb Removal efficiency %	Response 2 Fe Removal Efficiency %
1	767.09	7.91	4.08	41.50	46.66
2	767.09	4.08	4.08	55.69	50.22
3	431.82	1.80	6.36	46.20	46.64
4	767.09	4.08	4.08	49.50	50.60
5	1102.36	1.80	6.36	39.40	43.20
6	767.09	4.08	7.91	45.30	38.13
7	203.24	4.08	4.08	48.30	45.31
8	431.82	1.80	1.80	52.50	35.81
9	431.82	6.36	6.36	40.50	42.12
10	767.09	4.08	4.08	49.90	47.82
11	1102.36	6.36	6.36	51.50	44.10
12	767.09	0.25	4.08	34.90	42.50
13	767.09	4.08	0.25	48.70	38.43
14	1330.94	4.08	4.08	50.00	42.82
15	767.09	4.08	4.08	49.50	50.60
16	767.09	4.08	4.08	49.50	50.60
17	1102.36	6.36	1.80	49.20	44.20
18	431.82	6.36	1.80	44.10	40.91
19	1102.36	1.80	1.80	43.10	34.55
20	767.09	4.08	4.08	49.50	50.60

(Fig. not shown), this reduction shows that ion exchange and surface complexation may be the mechanism responsible for the uptake of Pb (II) and Fe (II) by the adsorbent [24].

Design of Experiments (DOE)

The optimized conditions for rice husk-spirogyra biosorbent were done with central composite design (CCD) in RSM using Design Expert 10.0.0®. The parameters considered were activation temperature (X_1), time (X_2) and mixing ratio (X_3) and they were done as factors 1, 2, 3 respectively, axial and center runs with the expected responses being Pb and Fe. The optimum conditions from the CCD analysis predicted for rice husk-spirogyra adsorbent gave values of activation temperature (X_1), activation time (X_2), and mixing ratio (X_3) to be 767.09 °C, 4.08 h, and 4.08 respectively, with 55.6 and 50.22% for optimum removal of Pb and Fe ions respectively as presented in Table 3.

Column adsorption

Column adsorption studies were carried out for adsorption of divalent cations of Fe(II) and Pb(II) onto rice husk–spirogyra adsorbent. The breakthrough time for each adsorbate was obtained. The column studies data were plotted to get the breakthrough curves which reflect the sorption behavior at definite time intervals on a fixed bed adsorption. This is presented as a plot of outlet concentration to the inlet concentration against time (Ct/C_0 versus time, t) as shown in Figs. 5, 6, and 7, respectively.

Effect of adsorbate inlet concentration

Fig. 5 shows the breakthrough curve for the removal of Fe(II) and Pb(II) at varying initial concentrations. The effect of inlet concentration of the adsorbate on the column performance was studied by varying the inlet concentrations of Fe
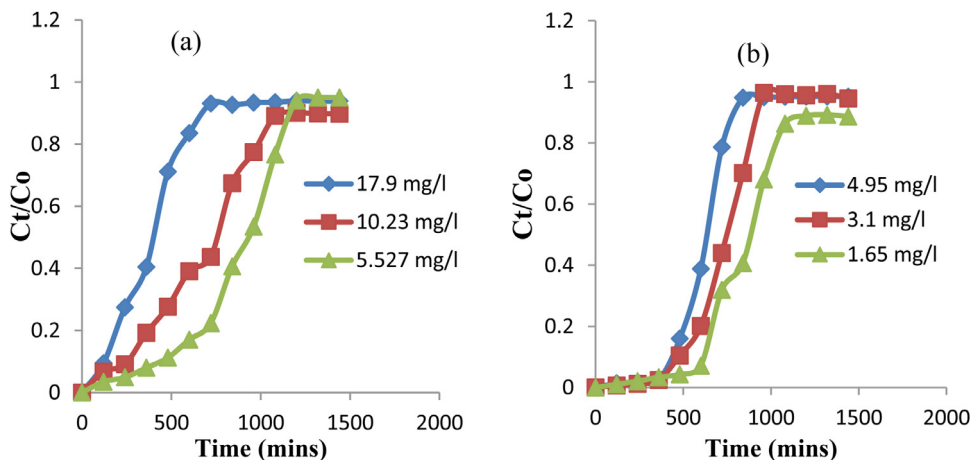
Fig. 5. Effect of adsorbate inlet concentrations at constant bed height of 7 cm and flow rate of 6 ml/min for (a) Fe (II) and (b) Pb (II) ions at varying time interval.
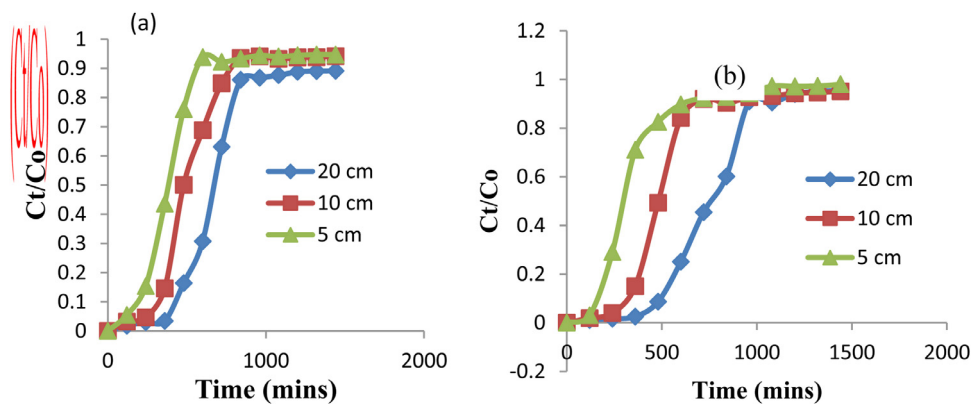
Fig. 6. Effect adsorbent bed heights at constant flow rate of 6 ml/min and initial ion concentrations for (a) Fe(II) and (b) Pb (II) at varying time interval.
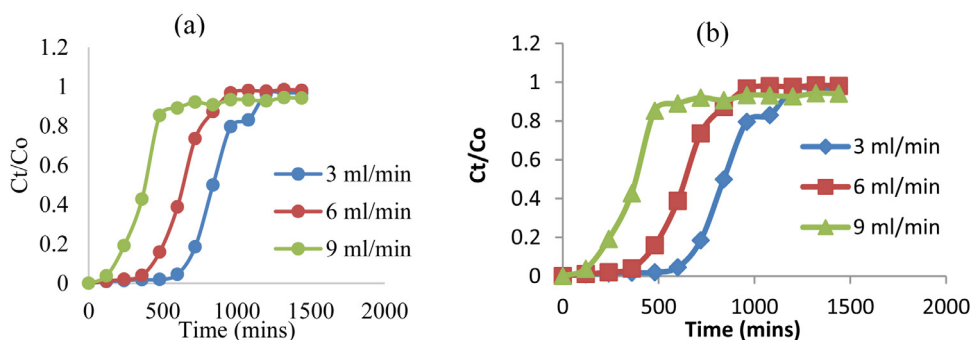
Fig. 7. Effect of flow rate at constant bed heights and initial ion concentrations for (a) Fe and (b) Pb (II) removal at varying time interval.

(II) at 17.9, 10.23 and 5.27 mg/L at constant bed height of 7 cm and feed flow rate of 6 ml/min. As seen from Fig. 5a breakthrough point ratio (Ct/Co) is the point at which the first adsorbate is detected at the output effluent and this was detected within the first 120 min, while bed saturation was attained after 1200 min. This equilibrate almost quickly when using the maximum initial concentration of 17.9 mg/L. Comparison at lower concentration of 5.27 mg/L and at the same (Ct/Co) value, it equilibrate at over 480 min. This can be ascertained from the curve; at an increasing influent concentration, the binding sites were occupied rapidly and the adsorbent bed get saturated at a shorter period of time. However, when the inlet concentration was decreased to 5.27 mg/L there was an extended breakthrough time and longer saturation time. Similar trend was observed from Fig. 5b for Pb (II). However, the breakthrough time was more extended for Pb(II) as the adsorbate had more affinity for the adsorbents than the Fe (II) [26].

Table 4
The R^2 Values of the linearized Clark model.

	R^2	A	r(L/min)
Fe(II) bed heights			
20 cm	0.8740	66.9200	0.0053
10 cm	0.8214	20.1590	0.0050
5 cm	0.7029	4.6057	0.0039
Pb(II) bed heights			
20 cm	0.9538	196.5900	0.0066
10 cm	0.7891	22.3700	0.0052
5 cm	0.7819	4.7403	0.0044
Fe(II) flow rate			
3 ml/min	0.9594	168.0400	0.0058
6 ml/min	0.7093	11.1241	0.0043
9 ml/min	0.4832	0.7850	0.0024
Pb(II) flow rate			
3 ml/min	0.9566	626.1500	0.0073
6 ml/min	0.9321	158.6000	0.0074
9 ml/min	0.6840	4.6640	0.0038
Fe(II) initial conc.			
17.90 mg/l	0.7701	3.6980	0.0035
10.23 mg/l	0.9594	19.4900	0.0041
5.27 mg/l	0.9643	85.8500	0.0053
Pb(II) initial conc			
4.95 mg/l	0.8537	108.5100	0.0065
3.10 mg/l	0.9125	270.2410	0.0071
1.65 mg/l	0.9550	211.5300	0.0058

Effect of bed height

Fig. 6 shows the breakthrough curve obtained for the adsorption of Fe (II) and Pb(II) on rice husk- Spirogyra adsorbent on three different bed heights of 5, 10 and 20 cm (with mass of 2.19, 4.9 and 7.1 g) respectively at constant effluent feed flow rate of 6 ml/min and an inlet concentration of 17.9 mg/L. From Fig. 6(a), at higher bed height, the curves tend to be less steep. Breakpoint (Ct/Co) and breakthrough time increased as the bed height is increased from 5 to 20 cm. This was validated from the results; at bed heights of 20 cm the first adsorbate was detected at over 480 min, while at 5 cm it was detected at 240 min. This is because at higher bed height, more adsorbents are present in the column, therefore more active sites resulting in greater uptake of the adsorbates. An increase in bed height would cause a larger distance for the mass transfer zone to arrive at the exit of the column [27]. Consequently, it would result in an extended breakthrough time. For higher bed heights, the increase of adsorbent mass would provide a larger service area leading to an increase in the volume of waste water to be treated. Similar trend to that is in Fig. 6(b), breakthrough curve was observed for Pb (II) at concentrations of 4.95 mg/L as seen from the plot; break through time increased when the bed height increased from 5 to 20 cm.

Effect of flow rate

Fig 7a shows the breakthrough curves at various flow rates of 3, 6 and 9 ml/min and at a constant bed height of 7 cm and initial concentration for Fe at 17.9 mg/L. It revealed that the breakthrough time generally occurred faster at higher flow rate. Breakthrough time decreased significantly when the flow rate was reduced to 3 ml/min and bed saturation took longer time. At a lower flow rate of influent, there were more contact with the adsorbent, which results in an improved removal of the heavy metals [28]. When the flow rate increased from 3 to 9 ml/min, the normalized concentrations ratio (Ct/Co) plots showed that the breakpoint time was reduced from 600 to 120 min at 3 to 9 ml/min respectively, while the bed exhaustion time decreased from over 1440 min to 360 min as well. Similar trend was observed on Fig. 7(b) for Pb (II) but at a more efficient removal.

Empirical model analysis

The empirical models Clark, Wolboska and Thomas models were used to predict the column behavior. Tables 4, 5 and 6 shows the values obtained for the linearized graphs of the Clark, Wolboska and Thomas model considered in this study. The results obtained revealed that the best fit for the column adsorption study was the Clark empirical model among other models studied as a result of their high R^2 values. The Clark model gave R^2 values of 0.9643 for Fe (II) ions and 0.9594 of Pb(II) ions respectively. For the Clark model it can also be observed that the value of A was highest for the largest bed hieght considered, indicating that the models fits the breakthrough curve behavior where the higher bed height is desirable for sorption.

The Wolboska model gave the highest R^2 values of 0.9627 for Fe(II) ions and 0.9078 of Pb(II) ions respectively. It can also be observed that the value of β_a was highest for the least flow rate considered 3 ml/min, indicating that the models fits the breakthrough curve behavior where lower flow rate is desirable for sorption [29].

Table 5
The R^2 values of the linearized Wolborska model.

	R^2	β_a l/h	N_o mg/L
Fe(II) bed height			
20 cm	0.7930	0.000155	0.7486
10 cm	0.6729	0.000240	1.5990
5 cm	0.5498	0.000320	3.2410
Pb(II) bed heights			
20 cm	0.8467	0.000185	0.2100
10 cm	0.6383	0.000260	0.4500
5 cm	0.4262	0.000310	0.8600
Fe(II) flow rate			
3 ml/min	0.9063	0.000520	2.0500
6 ml/min	0.6329	0.000310	2.2100
9 ml/min	0.3640	0.000114	2.2400
Pb(II) flow rate			
3 ml/min	0.9017	0.000610	0.5700
6 ml/min	0.7790	0.000500	0.6300
9 ml/min	0.5083	0.000230	0.6300
Fe(II) initial conc.			
17.9 mg/l	0.5941	0.000190	2.3200
10.23 mg/l	0.8692	0.000290	1.2000
5.27 mg/l	0.9627	0.000390	0.6200
Pb(II) initial conc.			
4.95 mg/l	0.7596	0.000500	0.6200
3.10 mg/l	0.8328	0.000500	0.3300
1.65 mg/l	0.9078	0.000530	0.1890

Table 6
The R^2 values of the linearized Thomas model.

	R^2	K_{th} L/mg.min	q_o mg/g
Fe(II) bed height			
20 cm	0.7930	0.0001750	13.068
10 cm	0.6729	0.0001356	17.410
5 cm	0.5498	0.0000904	24.000
Pb(II) bed height			
20 cm	0.8467	0.0008620	3.280
10 cm	0.6383	0.0006060	4.439
5 cm	0.4262	0.0006850	2.625
Fe(II) flow rate			
3 ml/min	0.9063	0.0001978	12.989
6 ml/min	0.6329	0.0001190	18.440
9 ml/min	0.3640	−0.0000450	4.450
Pb(II) flow rate			
3 ml/min	0.9017	0.0010000	0.326
6 ml/min	0.7790	0.0008160	5.540
9 ml/min	0.5083	0.0003230	5.030
Fe(II) initial conc.			
17.9 mg/l	0.5941	0.0000726	9.769
10.23 mg/l	0.8692	0.0001955	11.451
5.27 mg/l	0.9627	0.0019100	10.972
Pb(II) initial conc.			
4.95 mg/l	0.7596	0.0007010	6.572
3.10 mg/l	0.8328	0.0012900	4.318
1.65 mg/l	0.9078	0.0022400	2.474

The Thomas model gave the highest R^2 values of 0.9627 for Fe (II) ions and 0.9078 of Pb(II) ions respectively. For the Clark model it can also be observed that the value of K_{th} was highest for the largest bed hieght considered, indicating that the models fits the breakthrough curve behavior where the higher bed height is desirable for sorption [30].

Comparison with other adsorbents

Most of the adsorbents used in past studies showed that the adsorption was carried under batch process and the effluent treated were in minute quantities. The reverse is obtained in this study. The column continuous study, provides for larger volumes of highly polluted wastewater to be treated at optimum conditions using the modified rice husk ash spirogyra. This has helped to solve an environmental and community problem with ease [31-32]. The efficiency of the column study are on

Table 7
The Column Evaluation Performance for inlet concentration for both Pb and Fe (II).

Initial conc. (mg/l)	T_{total} (mins)	V_{eff}(ml)	M_{total} (mg)	q_{total} (mg)	Removal %	q_e(mg/g)
Fe (II)ions						
5.27	1200	7200	33.79	27.25	68.48	6.95
10.23	1080	6480	66.29	40.14	60.54	10.24
17.9	720	4320	77.33	37.34	48.29	9.53
Pb(II) ions						
1.65	1200	7200	13.07	8.21	62.80	2.09
3.1	960	5760	24.55	12.66	51.56	3.23
4.95	840	5040	8.91	5.19	58.30	1.33

Table 8
Comparison of adsorption capacity of Rice husk ash with other adsorbents.

Heavy metals	Adsorbents	Adsorption type	Removal Efficiency (%)	Adsorption capacity (mg/g)	References
Ni^{2+}, Zn^{2+}, Pb^{2+}, Cu^{2+} and Co^{2+} ions	Rice Husk Ash (RHA) and Rice Husk Ash derived Silica (RHS) and Triaminopropyl-Silica hybrid (TSH-R	Batch	99% and 95% for RHA and TSH-R		[33]
Fe(II) and Mn (II)	RHA	Batch		6.211 for Fe(II) ions and 3.016 for Mn(II) ions	[34]
Zn^{2+} and Pb^{2+}	Rice Husk	Batch	70% and 96.8% respectively.	19.67 and 0.6216 mg/g respectively	[35]
Pb (II)	Silical Gel composite from Rice husk ash modified 3-aminopropyltriothoxysilane (APTES)	Batch		46.9483	[36]
Pb, Cd, Cu, and Zn ions	Carbonized Rice Husk (CRH) and Activated Rice Husk (ARH)	Batch	54.3%, 8.24%, 51.4% and 56.7%, respectively using CRH, while it varied as 74.04%, 43.4%, 70.08% and 77.2% using ARH		[37]
Cu (II)	Spirogyra	Batch			[38]
Cu(II	alginate (Alg), algae waste biomass (AWB), and iron nanoparticles functionalized with alginate (Fe-NPs-Alg), and raw marine red algae biomass (RAB)	Batch	RAB (47.62 mg/g) < Fe-NPs-Alg (52.63) < AWB (83.33 mg/g) < Alg (166.66 mg/g).		[39]
Cd, Hg, and Pb	Macroalgae (sargassum crassifolium	Batch	75–99.05%		[40]
Cu, Fe, Co, Ni and Cr	S. crassifolium	Batch	< 56%		[40]
Cu^{+2}, Cr^{+3}, Cd^{+2} and Pb^{+2}	macroalga *Ulva lactuca* (AP) and its activated carbon (AAC) w	Batch	64.5 and 84.7 mg/g for Cu^{+2}, 62.5 and 84.6 mg/g for Cd^{+2}, 60.9 and 82 mg/g for $Cr+3$, and 68.9 and 83.3 mg/g for Pb^{+2}		[41]
Fe and Pb (II)	NaOH-rice husk ash spirogyra	Fixed bed column	48.29 and 58.30% of Fe and Pb (II)	9.53 and 1.33 mg/g for Fe and Pb (II)	This study

Table 7. At an industrial effluents concentration of 17.9 and 4.95 mg/L, 48.29 and 58.30% of Fe and Pb (II) were effectively removed amidst other competing ions and other water quality parameters.

The comparison of the literature results with using the rice husk or spirogyra independently and combining both are presented on Table 8.

Conclusion

This study has shown that the optimized rice husk-spirogyra adsorbent is a viable material for heavy metal removal in a column sorption process. The application of this adsorbent shows the extent of Pb(II) and Fe(II) removal based on the time it took to get its breakthrough which was set to their standard limits in the environment. The Rice husk-spirogyra adsorbent was characterized before and after adsorption with FT-IR, SEM, TGA and BET surface analyzer. The FT-IR showed that the functional group responsible for the adsorption are the hydroxyl group, carboxylic and carbonyl groups. The BET results revealed a large surface area which decreased after the adsorption process, the SEM revealed presence of pores and an irregular rough surface which showed swellings after sorption and EDX confirmed the appearance of Pb and Fe (II) ions on the peaks. The optimum conditions for developing the rice husk-spirogyra adsorbent were activation temperature of 767.09 °C, time of 4.08 h and at a mixing ratio of 4.08. The parametric evaluation of the bed height, flow rate and initial concentration showed that an increase in bed heights, reduced flow rates and inlet concentrations had a significant effect on the breakthrough time and bed exhaustion time. The column efficiency results at optimum condition treated over 4000 mL of polluted wastewater with over 50% removal efficiency for both ions and a bed capacity of 12.48 and 1.21 mg/L for Fe and Pb (II) respectively. The Clark empirical model best fit with the experimental data's with R^2 values of 0.9643 for Fe(II) ions and 0.9594 of Pb(II) ions.

Declaration of Competing Interest

The Author's declared that there is no conflict of interest.

Funding statement

References

[1] K.S. Obayomi, M. Auta, Development of microporous activated Aloji clay for adsorption of Pb(II) from aqueous solution, Heliyon 5 (2019) (2019) e02799.
[2] S.K. Chatterjee, I. Bhattacharjee, G. Chandra, Biosorption of heavy metals from industrial waste water by Geo bacillus thermos denitrificans, J. Hazard. Mater. 175 (2010) 117–125.
[3] M.D. Yahya, K.S. Obayomi, M.B. Abdulkadir, Y.A. Iyaka, A.D. Olugbenga, Adsorption equilibrium study on the characterization of cobalt-ferrite supported on activated carbon for the removal of chromium and lead ions from tannery wastewater, Water Sci. Eng. (2020), doi:10.1016/j.wse.2020.09.007.
[4] K.S. Obayomi, J.O. Bello, M.D. Yahya, E. Chukwunedum, J.B. Adeoye, Statistical analyses on effective removal of cadmium and hexavalent chromium ions by multiwall carbon nanotubes (MWCNTs), Heliyon 6 (2020) e04174, doi:10.1016/j.heliyon.2020.e04174.
[5] K. Vijayaraghavan, R. Balasubramanian, Is bio sorption suitable for decontamination of metal-bearing wastewaters? A critical review on the state-of-the-art of bio sorption processes and future directions, J. Environ. Manage. (2015) 1–14.
[6] R. Vimala, D. Charumathi, D. Nilanjana, Packed bed column studies on Cd (II) removal from industrial wastewater by macro fungus Pleurotus platypus, Desalination 275 (2011) 291–296.
[7] M.D. Yahya, A.S. Aliyu, K.S. Obayomi, A.G. Olugbenga, U.B. Abdullahi, Column adsorption study for the removal of chromium and manganese ions from electroplating wastewater using cashew nutshell adsorbent, Cogent Eng. 7 (1) (2020) 1748470.
[8] T. Kornboonraksa, H. Lee, S.H. Lee, C. Chiemchaisri, Application of chemical precipitation and membrane bioreactor hybrid process for piggery waste water treatment, Bioresour. Technol. 3 (2009) 348–357.
[9] J. Patel, Ion Exchange Resins, Researchgate 1 (51) (2016) 12–25.
[10] L. Castro, M. Luis, G. Felisa, A. Jesús, B. Antonio, Bio sorption of Zn (II) from industrial effluents using sugar beet pulp and F. vesiculosus: from laboratory tests to a pilot approach, Sci. Total Environ. 598 (2017) 856–866.
[11] T.K. Naiya, P. Chowdhury, A.K. Bhattacharya, S.K. Das, Saw dust and Neem bark as low-cost natural biosorbent for adsorptive removal of Zn(II) and Cd(II) ions from aqueous solutions, Chem. Eng. J. 148 (2009) 68–79.
[12] K.S. Obayomi, J.O. Bello, J.S. Nnoruka, A.A. Adediran, P.O. Olajide, Development of low- cost bio-adsorbent from agricultural waste composite for Pb(II) and As(III) sorption from aqueous solution, Cogent Eng. 6 (2019) 1687274.
[13] M.D. Yahya, K.S. Obayomi, B.A. Orekoya, A.G. Olugbenga, B. Akoh, Process evaluation study on the removal of Ni(II) and Cu(II) ions from an industrial paint effluent using kola nut pod as an adsorbent, J Dispers Sci Technol (2020), doi:10.1080/01932691.2020.1822178.
[14] M.D. Yahya, I. Yohanna, A. Auta, K.S. Obayomi, Remediation of Pb (II) ions from Kagara Gold Mining Effluent using Cotton Hull Adsorbent, Sci. Afr. 8 (2020) e00399, doi:10.1016/j.sciaf.2020.e00399.
[15] K.S. Obayomi, M. Auta, A.S. Kovo, Isotherm, kinetic and thermodynamic studies for adsorption of lead (II) onto modified Aloji clay, Desalination Water Treat 181 (2020) 376–384.
[16] A. Chatterjee, A. Jayanthi, Biosorption Capacity of Dried Spirogyra on Heavy Metals, Int. J. Chemtech. Res. 8 (2015) 387–392.
[17] T. Barbosa, E.L. Foletto, Preparation of mesoporous geopolymer using metakaolin and rice husk ash as synthesis precursors and its use as potential adsorbent to remove organic dye from aqueous solutions, Ceram Int. 44 (2017) 416–423.
[18] D. Yadav, K. Meghna, K. Pradeep, Adsorptive removal of phosphate from aqueous solution using rice husk and fruit juice residue, Process. Saf. Environ. Protect. (2014) 482 8.2018 Edition of the Drinking water standards and health advisories EPA,822-18-001.
[19] L.T. Popoola, A.A. Tajudeen, Synthesis of composite snail shell- rice husk adsorbent for brilliant green dye uptake from aqueous solution: optimization and characterization, Biomed Res Int 51 (1) (2019) 12–25.
[20] O. Ekpete, M. Horfsal, Preparation and Characterization of Activated Carbon derived from Fluted Pumpkin Stem Waste, Res. J. Chem. Sci. 12 (2) (2011) 125–130.
[21] F. Colak, A. Necip, Y. Demet, O. Asim, Biosorption of lead from aqueous solutions by Bacillus strains possessing heavy-metal resistance, Chem. Eng. J. 173 (2011) 422–428.
[22] A.O. Dada, A.P. Olalekan, A.M. Olatunya, Langmuir, Freundlich, Temkin and Dubinin–Radushkevich Isotherms Studies of Equilibrium Sorption of Zn^{2+} Unto Phosphoric Acid Modified Rice Husk, IOSR J. Appl. Chem. 3 (2012) 38–45.
[23] N. Alias, I. Norazana, A. Kamaruddin, Thermogravimetric Analysis of Rice Husk and Coconut Pulp for Potential Biofuel Production by Flash Pyrolysis, Ceram Int 3 (2) (2014) 108–114.
[24] J. Singh, A. Ali, V. Prakash, Removal of lead (II) from synthetic and batteries wastewater using agricultural residues in batch/column mode, Int. J. Environ. Sci. Technol. 11 (2014) 1759–1770.

[25] M.D. Yahya, C.V. Ihejirika, Y.A. Iyaka, U. Garba, A.G. Olugbenga, Continuous sorption of chromium ions from simulated effluents using citric acid modified sweet potato peels, Nig. J. Technol. Dev. 17 (1) (2020) 47–53.

[26] S.O. Lesmana, N. Febriana, F.E. Soetaredjo, J. Sunarso, S. Ismadji, Studies on potential applications of biomass for the separation of heavy metals from water and wastewater, Biochem. Eng. J. 44 (2009) 19–41.

[27] I. Anastopoulos, G.Z. Kyzas, Progress in batch biosorption of heavy metals onto algae, J. Mol. Liq. 209 (2015) 77–86.

[28] A. Esmaeili, A. Beni, Optimization and design of a continuous biosorption process using brown algae and chitosan/PVA nano-fiber membrane for removal of nickel by a new biosorbent, Int. Journal Environ. Sci. Technol. (2017) 1–14.

[29] M.A . Cechinel, Removal of metal ions from a petrochemical wastewater using brown macro-algae as natural cation exchangers, Chem. Eng. J. 286 (2016) 1–15.

[30] A. Esmaeili, A. Beni, A novel fixed-bed reactor design incorporating an electrospun PVA/chitosan nanofiber membrane, J. Hazard. Mater. 280 (2014) 788–796.

[31] Y. Shang, X. Yu, Screening of algae material as a filter for heavy metals in drinking water, Algal Res 12 (2015) 258–261.

[32] D.M.R.E. Dissanayake, W.M.K.E.H. Wijesinghe, S.S. Iqbal, N. Priyantha, M.C.M. Iqbal, Isotherm and kinetic study on Ni(II) and Pb(II) biosorption by the fern Asplenium nidus L, Ecol Eng 88 (2016) 237–241.

[33] F.J. Ligate, J.E.G. Mdoe, Removal of heavy metal ions from aqueous solution using rice husks-based adsorbents, Tanzan. J. Sci. 41 (2015) 1–13.

[34] Y. Zhang, J. Zhao, Z. Jiang, D. Shan, Y. Lu, Biosorption of Fe(II) and Mn(II) Ions from Aqueous Solution by Rice Husk Ash, Biomed. Res. Int. (2014) 10, doi:10.1155/2014/973095.

[35] A. Elham, T. Hossein, H. Mahnoosh, Removal of Zn(II) and Pb (II) ions using rice husk in food industrial wastewater, J. Appl. Sci. Environ. Manage. 14 (4) (2010) 159–162.

[36] A.P. Yusmaniar, A.E. Putri, D. Rosyidah, Adsorption of Pb(II) Using Silica Gel Composite from Rice Husk Ash Modified 3-aminopropyltriethoxysilane (APTES)- activated carbon from coconut shell, AIP Conf Proc 1823 (2017) 020034, doi:10.1063/1.4978107.

[37] I. Nhapi, N. Banadda, R. Murenzi, C.B. Sekomo, U.G. Wali, Removal of heavy metals from industrial wastewater using rice husks, Open Environ. Eng. J. 4 (2011) 170–180 2011.

[38] Z. Al-Qodah, E. Assirey, Bioadsorption of Copper from wastewater by Algal Biomass, Res. Gate (2019) 1–28.

[39] A.R. Lucaci, D. Bulgariu, M. Popescu, L. Bulgariu, Adsorption of Cu(II) ions on adsorbent materials obtained from marine red algae *Callithamnion corymbosum sp*, Water (Basel) 12 (372) (2020) 1–16, doi:10.3390/w12020372.

[40] L. Surayya, Eka. Putri, E Syafiqa, The adsorption of heavy metals from industrial wastewater using sargassum crassifolium, Int. J. GEOMATE 17 (59) (2019) 21–27, doi:10.21660/2019.59.4603.

[41] W.M. Ibrahim, A.F. Hassan, Y.A. Azab, Biosorption of toxic heavy metals from aqueous solution by Ulva lactuca activated carbon, Egypt. J. Basic Appl. Sci. 3 (2016) 241–249, doi:10.1016/j.ejbas.2016.07.005.